



HAL
open science

A stochastic method to propagate uncertainties along large cores deterministic calculations

Ludovic Volat, Bernard Gastaldi, Alain Santamarina

► **To cite this version:**

Ludovic Volat, Bernard Gastaldi, Alain Santamarina. A stochastic method to propagate uncertainties along large cores deterministic calculations. *European Journal of Physics*, In press. cea-01597850v1

HAL Id: cea-01597850

<https://cea.hal.science/cea-01597850v1>

Submitted on 28 Sep 2017 (v1), last revised 29 Jun 2018 (v2)

HAL is a multi-disciplinary open access archive for the deposit and dissemination of scientific research documents, whether they are published or not. The documents may come from teaching and research institutions in France or abroad, or from public or private research centers.

L'archive ouverte pluridisciplinaire **HAL**, est destinée au dépôt et à la diffusion de documents scientifiques de niveau recherche, publiés ou non, émanant des établissements d'enseignement et de recherche français ou étrangers, des laboratoires publics ou privés.

A STOCHASTIC METHOD TO PROPAGATE UNCERTAINTIES ALONG LARGE CORES DETERMINISTIC CALCULATIONS

Ludovic Volat¹, Bernard Gastaldi¹, and Alain Santamarina¹

CEA, DEN, DER, SPRC, Cadarache 13108 Saint-Paul Les Durance Cedex

Received: date / Revised version: date

Abstract. Several evolutionary advanced nuclear reactors, whose operational life is intended to be 60 years, are currently being built throughout the world. Deterministic uncertainty propagation methods are certainly powerful and time-sparing but their access to uncertainties related to the power map stays difficult due to a lack numerical convergence. On the contrary, stochastic methods facilitate the propagation of uncertainties related to the core power map and they enable a more rigorous access to those concerning the prompt fission neutron spectrum. In this sense, they supplement previous studies. Our method combines an innovative calculation chain and a stochastic way of propagating uncertainties on nuclear data : first, our calculation scheme consists in the calculation of assembly self-shielded cross sections and a flux calculation on the whole core. Bias is quantified and the CPU time needed is suitable to lead numerous calculations. Then, we sample nuclear cross sections with consistent probability distribution functions with a correlated sampling. Finally, we deduce the power map uncertainties from the study of the output response functions. We performed our study on the system described in the framework of the OECD/NEA Expert Group in Uncertainty Analysis in Modelling (UAM). Results show ^{238}U inelastic scattering, the ^{235}U PFNS and the ^{26}Fe cross sections as major contributors of the total uncertainty on the power map whose value is 3% (1σ) with the COMAC covariance library.

PACS. key describing text of that key – PACS-key describing text of that key

1 Introduction

1.1 Context GEN III cores

The improvements in reactor technology of the so-called GEN-III reactors are intended to result in a longer operational life (at least 60 years of operation) compared with currently used GEN-II reactors (designed for 40 years of operation). In particular, they take advantage from a simpler and more rugged design, making them easier to operate and less vulnerable to operational upsets. From a neutronic point of view, a higher burn-up is accepted to reduce fuel use as well as the amount of corresponding waste. More specifically, we will study PWRs cores part of the Generation-III which are bigger than those of GEN-II.

1.2 Objectives

Whilst powerful and time - sparing methods have been largely used to propagate uncertainties in core calculations [1], a great endeavour is made to brush up on brute force methods. Actually, thanks to growing calculation means, stochastic methods become more attractive to calculate the uncertainty introduced by simulation codes. These methods consist in taking into account the uncertainties either since the very beginning of the calculation chain [2] or by sampling nuclear cross sections with consistent probability distribution functions [3]. Having regard to the nuclear model parameters uncertainty ranges one can process nuclear data libraries (for example with TALYS [4]). Finally, the uncertainties are deduced from the study of the output parameters of interest distribution function.

Here, we propose a similar method which combines an innovative calculation chain and a stochastic way of propagating uncertainties on nuclear data. Given that larger cores are more sensitive to an external perturbation, the uncertainties associated with calculation parameters and design dimensions are worth studying. We propose then here to propagate uncertainties due to nuclear data on LWR key parameters such multiplication factor and core power map.

1.3 Theoretical background

The Boltzmann equation, which translates the neutron balance in a nuclear reactor, can be written in a compact form as

$$(A_0 - \lambda_0 F_0)\phi_0 = 0 \quad (1)$$

where A_0 is the disappearance operator, F_0 the neutron production operator, ϕ_0 is the unperturbed neutron flux and $\lambda_0 = 1/k_0$ with k_0 the first eigenvalue associated with the fundamental mode flux ϕ_0 . Theoretical arguments lead to express a perturbed flux sensitivity coefficient a_1 as following

$$a_1 = \frac{1}{\underbrace{\lambda_1 - \lambda_0}_{=EVS}} \frac{\langle \phi_1^\dagger | (\lambda_0 \delta F - \delta A) \phi_0 \rangle}{\langle \phi_1^\dagger | F_0 \phi_1 \rangle} \quad (2)$$

where $\lambda_1 = 1/k_1$ is the inverse of the first harmonic eigenvalue of the flux. While the scalar product is dependent on the external perturbation only, the first term is directly related to the size of the core. $\frac{1}{\lambda_1 - \lambda_0}$ is called the Eigenvalue Separation Factor (EVS) and grows like the size of the core. Thus, with the same initial perturbation,

the larger is the core, the higher will be the resulting flux perturbation amplitude. The deterministic nuclear data uncertainty propagation on a manifold sample of french PWRs (from 900 MWe up to 1700 MWe) showed that the central assembly power uncertainty increases from 1.5% to 4% (1σ)[5] mainly due to the uncertainty on U238 inelastic scattering.

2 The core calculation scheme

2.1 Physical model

Our model is based on a sample proposed in the framework of the Working Party on International Nuclear Data Evaluation Co-operation (WPEC) of the OECD/Nuclear Energy Agency[6]. An international numerical benchmark has been proposed to study the uncertainties related to large cores : a fresh core with 241 assemblies, each of them containing 265 pins. We consider a situation at Hot Zero Power. A whole 2D core calculation is undertaken, with a refined pin description and a flux calculation scheme in two steps. First, each individual assembly geometry in an infinite lattice is described and self-shielded 281 SHEM [7] energy groups cross sections are produced. Then, the neutron flux is calculated thanks to the Method of Characteristics (MOC) onto the whole geometry. Even though the computational power has been steadily growing with time, yet the CPU time needed in order to have flux convergence is still too high. That is why several assumptions are made in order to reduce CPU time cost. Given that the steady state Boltzmann equation is discretized

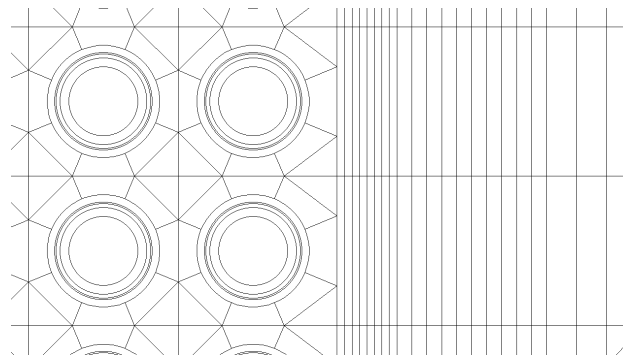


Fig. 1. Spatial Core Mesh : Interface between the peripheral assemblies and the heavy reflector

in space and energy, we decided to make the calculation parameters vary from the industrial calculation routine *APOLLO2.8/CEA2005V4* usually used at CEA [8].

- In terms of angular discretization of the flux, we decided to work with conventional P3 calculation.
- Concerning the space discretization of the characteristics tracking, we chose to work with a refined mesh, imposing a distance between each characteristic which amounts to an order of magnitude of 0.04cm.
- We present in Fig.1 the spatial mesh of our study. The interface between the reflector and the peripheral assembly has been highly meshed to keep a good description of the impact of the reflector on the power map. [9]
- Finally, we used the 20 groups energy mesh [8] cf. Table 1 for the core flux calculation which is optimized for LWR calculations.

In short, our simplified scheme consists in two parts :

1. Calculation of self-shielded cross sections above 23eV for each assembly and determination of the 281g flux spectrum (SHEM mesh) using Pij method.

Group	Energy upper bound	Comments
1	19.64 MeV	(n,2n) and 2 nd chance fission
2	4.490 MeV	Fast domain
3	2.231 MeV	First resonance of ¹⁶ O
4	1.337 MeV	
5	494 eV	
6	195 keV	
7	67.38 keV	
8	25 keV	
9	9.12 keV	Unresolved domain
10	1.91 keV	
11	411 eV	Resolved resonances
12	52.67 eV	3 first resonances of ²³⁸ U
13	4.000 eV	²⁴⁰ Pu & ²⁴² Pu resonances
14	625 meV	
15	353 meV	Resonances of ²³⁹ Pu
16	231.2 meV	
17	138 meV	
18	76.5 meV	Purely thermal domain
19	34.4 meV	
20	10.4 meV	

Table 1. Description of the 20 groups energy mesh

2. Flux calculation (MOC) on the core with collapsed 20 group cross-sections.

Our method allowed to reduce the CPU cost from 1 day to 1 hour, on a single Intel 3GHz processor with 11Go of RAM use.

3 The cross sections sampling method

The covariance input data file are given in terms of mean values and standard deviation. We choose to model the input uncertainty as a gaussian probability density function with the mean and standard deviation given by our covariance library. Given that the number of calculations is limited, the population of our statistical sample must be small. This so-called Design of Experiments must be then wisely chosen in order to fulfill the three following properties : optimal covering of the input parameter space, robustness of projections over 2D subspaces and sequentiality. Now, we will show that the Latin Hypercube Sampling is the optimum fitting to our need. The LHS sampling comes down to equally chop off all the dimensions, and thus make sub-intervals of equal bin width. Each sampling point coordinate is the only one in each sub-interval. Then, due to the non-uniqueness of a LHS for a given dimension and population, a optimization criterion must be found in order to get the best LHS with the smallest population. We show in Fig. 2 the efficiency of the estimator associated to the mean of the effective multiplication factor (k_{eff}) for different ways of producing and optimizing our LHS design of experiments. The L2star discrepancy optimization and C2 discrepancy optimization have already been largely described in [10]. Even though we can see here that it gives a better efficiency of the estimator at small populations, the limiting criterion to choose the best population is the empirical standard deviation of the mean of the k_{eff} (right -hand side of the figure). In order to get the best compromise between a low standard devi-

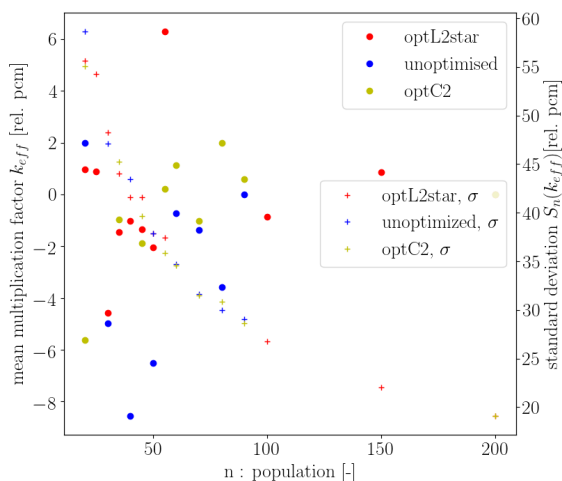


Fig. 2. Estimators convergence function of the population

ation and a limited population, we chose a population of 50 with a L2-star optimized LHS. Once we sampled each cross section in each energy group as a gaussian $\mathcal{N}(0, 1)$, covariance libraries have to be taken into account. This was made by using a Cholesky-type decomposition. Here we note the covariance matrix C , the dimension of our problem d , the vector containing all the means $\vec{\mu}$. We are looking for a multivariate gaussian vector $Y \in \mathcal{R}^d$, whose probability density function (pdf) is $\mathcal{N}(\vec{\mu}, C)$ with $\vec{\mu}$ the vector of the means along all dimensions. Let us note $Y = QX + \vec{\mu}$. The problem is actually equivalent to choose Q so that $\mathbb{E}(Y^t Y) = C$. We took eventually Q as $Q = PD^{1/2}$ where D is the eigenvalues diagonal matrix of C and P the corresponding transfer matrix. In the frame composed by the eigenvectors, the linear application corresponding to $D^{1/2}$ is a dilatation of the distribution and P corresponds to a rotation. Then the distribution is shifted by $\vec{\mu}$.

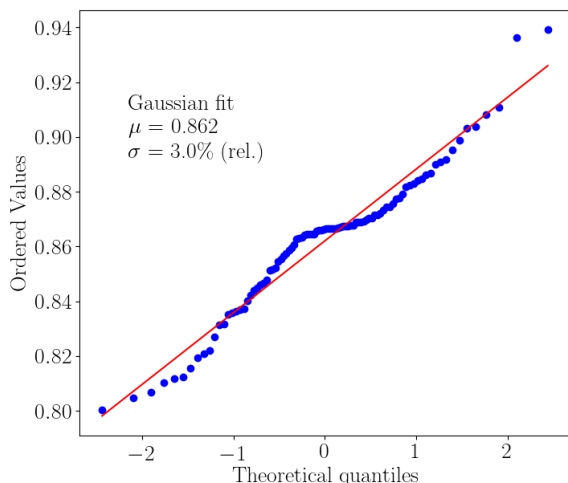


Fig. 3. Probability plot to deduce the uncertainty related to the center of the power map, COMAC V2

4 Results

The cross-section values calculated during the self-shielding step are modified according to Y . Then, for each sampling, our calculation routine is run. Then we study the final distribution function of the multiplication factor and the one of the assembly power map in order to deduce the associated uncertainties. The gaussian output function is inferred by fitting the probability plot, like shown in Fig. 3.p For this work, we chose to use two sets of covariances matrices taken from COMAC : the first one, called here COMAC V0 [11], was released in 2012 and the second one, called COMAC V2 contains major results obtained until 2016 [12], [13]. Thus, we want to compare the impact of the two libraries on the power map and highlight how the library change has contributed to reduce the contribution of several major isotopes to the total uncertainty. Figure 2 spots the majors contributions to the total uncertainty on the k_{eff} , the center of the power map, and the pe-

Contributor rank	unc. k_{eff}	pcm	unc. P_{center}	std	unc. $P_{periph. ass.}$	std
1	$^{238}U (n, f)$	409	$^{235}U \chi$	2.4%	$^{235}U \chi$	2.0%
2	$^{238}U (n, \gamma)$	312	$^{238}U (n, n')$	2.0%	$^{238}U (n, n')$	1.5%
3	$^{235}U \bar{\nu}$	273	$^1H(n, n)$	1.2%	$^1H(n, n)$	1.1%
4	$^{235}U \chi$	215	$_{26}Fe(n, n)$	0.7%	$_{26}Fe(n, n)$	0.8%
5	$^{235}U (n, f)$	147	$^1H(n, \gamma)$	0.3%	$^{238}U (n, f)$	0.4%
6	$^{235}U (n, \gamma)$	143	$^{238}U (n, \gamma)$	0.3%	$^{238}U (n, \gamma)$	0.3%
Total uncertainty	k_{eff}	737	P_{center}	3.6%	$P_{periph. ass.}$	2.8%

Table 2. Main contributors and total propagated uncertainty (1σ) with COMAC V0

	unc. k_{eff}	pcm	unc. P_{center} and unc. $P_{periph. ass.}$
1	$^{235}U \bar{\nu}$	277	$^{238}U (n, n')$ 0.8%
2	$^{238}U (n, \gamma)$	248	$^{235}U \chi$ 0.8%
3	$^{235}U (n, \gamma)$	145	$_{26}Fe(n, n)$ 0.8%
4	$^{235}U (n, f)$	144	$^{235}U (n, \gamma)$ 0.3%
5	$^1H(n, \gamma)$	132	$^{238}U (n, \gamma)$ 0.3%
6	$^{238}U (n, f)$	116	$^1H(n, n)$ 0.3%
7	$^{235}U \chi$	103	$^1H(n, \gamma)$ 0.3%
Total uncertainty	k_{eff}	634	$P_{center} : 3\%$ $P_{periph. ass.} : 2.3\%$

Table 3. Main contributors and total propagated uncertainty (1σ) with COMAC V2

ripheral assemblies. Those two latters contain the highest uncertainties of the power map. Results show that the calculated total uncertainty on the k_{eff} stands at 737 pcm, on the center of the map 3.6% and on the last ring of assemblies 2.8%. Similarly, Table. 4 presents the last results obtained with the new covariance library, COMAC V2.

- The contribution due to the ^{238}U fission cross section has dramatically been reduced : above 1 MeV, the standard deviation in COMAC V2 has been taken to be around 2-3%, the same order of magnitude as the

standards. That leads to a reduction of its contribution by a factor 4 on the k_{eff} .

- Concerning the contribution of the inelastic cross section of ^{238}U , the uncertainty value above the threshold has been taken at around 15%, as the value given in JENDL-4.0. These values stay much lower than the one given *e.g.* by ENDF.VII.1 (30%). Anyway, the importance of this uncertainty has been proven in recent work. That is why latests evaluations and experimen-

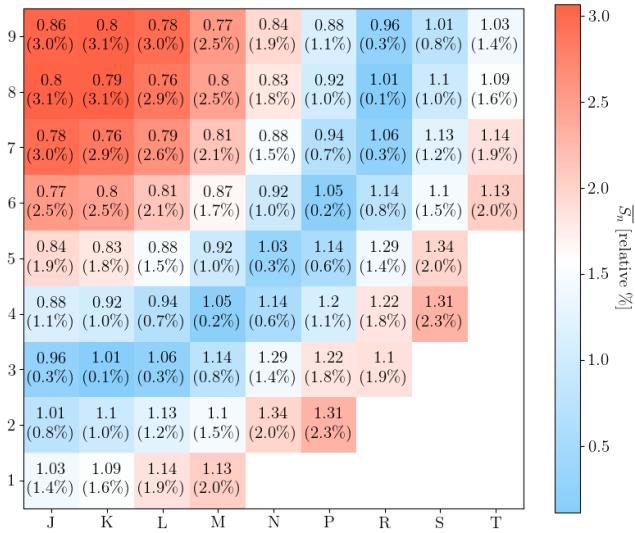


Fig. 4. Normalized Power Map with uncertainties (1σ) underneath

tal measurements contributed very recently to reduce it even more [14].

- The contribution of the ^{235}U PFNS uncertainty has been reduced : the niveau of the input uncertainty has been reduced by more than a factor 2 on the whole energy range, reducing drastically the uncertainty on the power map.
- Concerning the contribution of the (n, n) of ^1H , COMAC V0 suggest an increase of the uncertainty above 70keV. However, by conservation of the whole uncertainty, the value at high energies should be much lower [15]. It was then taken into account in COMAC V2.

Finally, the Fig. 4 shows the whole uncertainty map on our core. It shows then clearly the radial swing between the centre and the last ring of assemblies.

5 Summary and Conclusions

Through this, we proved that uncertainties on LWR parameters due to nuclear data can be propagated through a brute force method thanks to enhanced and enlarged calculation means. This method gives access to all of the needed uncertainties without developing any dedicated perturbation theory or using special hypothesis.

We applied this method to a PWR large core NEA benchmark and showed that the overall k_{eff} uncertainty reaches 634 pcm, 3% for the centre of the power map and 2.3% for the last ring of assemblies. The main contributors are $\bar{\nu}$, the capture and fission cross sections of ^{235}U , the capture cross section of ^{238}U for the k_{eff} . Inelastic scattering of ^{238}U , PFNS of ^{235}U and elastic scattering of $_{26}\text{Fe}$ are the main contributors to the assembly power. This method could be then applied to propagate other uncertainties, especially design and technological uncertainties, whose analytical expressions are difficult to derive.

6 Acknowledgments

The authors would like to thank CEA's industrial partners Electricité de France and AREVA for their financial support to this work.

References

1. A. Gandini. A generalized perturbation method for bilinear functionals of the real and adjoint neutron fluxes. *Journal of Nuclear Energy*, 21(10):755–765, October 1967.

2. A.J. Koning and D. Rochman. Towards sustainable nuclear energy: Putting nuclear physics to work. *Annals of Nuclear Energy*, 35(11):2024–2030, November 2008.
3. W. Zwermann, Krzykacz-Hausmann B., Gallner L., Pautz A., and Mattes M. Uncertainty Analyses with Nuclear Covariance Ddata in Reactor Core Ccalculations. *Journal of the Korean Physical Society*, 59(23):1256, August 2011.
4. A.J. Koning and D. Rochman. Modern Nuclear Data Evaluation with the TALYS Code System. *Nuclear Data Sheets*, 113(12):2841–2934, December 2012.
5. Alain Santamarina, Patrick Blaise, Nicolas Dos Santos, Claire Vaglio-Gaudard, and Cyrille De Saint Jean. Nuclear data uncertainty propagation on power maps in large LWR cores. In *JAEA-Conf-2014-003*, Japan, 2015.
6. K. Ivanov, M. Avramova, and S. Kamerow. *Benchmarks for uncertainty analysis in modelling (UAM) for the design, operation and safety analysis of LWRs*, volume 1 : Specification and Support Data for Neutronics Cases (Phase I). OECD, NEA, May 2013.
7. N. Hfaiedh and A. Santamarina. Determination of the optimised SHEM mesh for neutron transport calculation. *Proc. Int. Conf. on Mathematics and Computation*, 2005.
8. Alain Santamarina, David Bernard, Patrick Blaise, Pierre Leconte, Jean-Marc Palau, Bénédicte Roque, Claire Vaglio, and Jean-François Vidal. Validation of the new code package APOLLO2.8 for accurate PWR neutronics calculations. In *Validation of the new code package APOLLO2.8 for accurate PWR neutronics calculations*, Sun Valley, Idaho, USA, May 2013. ANS.
9. A. Sargeni, K.W. Burn, and G.B. Bruna. The impact of heavy reflectors on power distribution perturbations in large PWR reactor cores. *Annals of Nuclear Energy*, 94:566–575, August 2016.
10. G Damblin, M Couplet, and B Iooss. Numerical studies of space-filling designs: optimization of Latin Hypercube Samples and subprojection properties. *Journal of Simulation*, 7(4):276–289, November 2013.
11. Cyrille De Saint Jean. Estimation of multi-group cross section covariances for 235,238 U, 239 Pu, 241 Am, 56 Fe, 23 Na and 27 Al. Knoxville, Tennessee, USA, April 2012. ANS.
12. Léonie Berge. *Contribution à la modélisation des spectres de neutrons prompts de fission. Propagation d'incertitudes sur un calcul de fluence cuve*. PhD thesis, Grenoble-Alpes, Grenoble, July 2015.
13. Nicholas Terranova. *Covariance Evaluation for Nuclear Data Interest to hte Reactivity Loss Estimation of the Jules Horowitz Material Testing Reactor*. PhD thesis, Université de Bologne, Bologne, 2016.
14. A. Santamarina, D. Bernard, P. Leconte, and J.-F. Vidal. Improvement of 238U Inelastic Scattering Cross Section for an Accurate Calculation of Large Commercial Reactors. *Nuclear Data Sheets*, 118:118–121, April 2014.
15. David Bernard. Personal Communication, 2016.